ORGANIC PROCESS RESEARCH & DEVELOPMENT
OPR&D

pubs.acs.org/OPRD

Review

Targeting Particle Size Specification in Pharmaceutical Crystallization: A Review on Recent Process Design and Development Strategies and Particle Size Measurements

Fan Liu,* Sujay D. Bagi, Qinglin Su, Rajshree Chakrabarti, Rita Barral, Janaka C. Gamekkanda, Chuntian Hu, and Salvatore Mascia*

Cite This: https://doi.org/10.1021/acs.oprd.2c00277

Read Online

ACCESS | Metrics & More | Article Recommendations

ABSTRACT: Obtaining a particle size within the specifications for a pharmaceutical compound in an industrial crystallization can be a challenging task. The events affecting the final particle size of the product include nucleation, growth, breakage, and agglomeration, which are often convoluted. Secondary nucleation may significantly influence the particle size distribution. The strategies and techniques relevant to obtaining an in-spec particle size in crystallization are summarized and discussed from a perspective of process parameters. The effect of cooling profiles, seeding strategies, as well as mixing by agitation are reviewed, and an efficient and controlled crystallization process may be achieved using an optimized combination of these conditions. Multiple characterization methods for particle size and distribution are compared, and the discrepancies associated with the measurements are addressed.

KEYWORDS: *cooling crystallization, large particle sizes, seeding, kinetics, particle size distribution*

1. INTRODUCTION

The goal of the crystallization process in the pharmaceutical industry is to isolate the drug substances and intermediates as solid materials with targeted product attributes. The physical properties of the solids, e.g., crystallinity, purity, mechanical properties, particle size, and shape, play an important role in the development and production of pharmaceuticals.[1−4] The U.S. Food and Drug Administration (FDA) defines critical quality attributes (CQA) as physical, chemical, biological, or microbiological properties or characteristics that should be within an appropriate limit, range, or distribution to ensure the desired product quality.[5] CQAs are generally associated with the drug substance (also referred to as active pharmaceutical ingredient, API), excipients, intermediates (in-process materials), and drug product. Particle size is a common CQA of drug substances as it affects downstream processability and drug release characteristics. Achieving the desired particle size can often be challenging owing to the interplay among various process parameters. Substantial efforts have been made to tune the particle size as the targeted product attribute during the process development of crystallization. A series of techniques, including mathematical modeling tools, have been applied for the prediction and control of particle size and distribution.[6−11]

A large particle size can be the targeted quality attribute for a drug compound. Large particles generally have good flowability and avoid the issues created by small particles, e.g., clogging during a filtration step. The general observation is that the large particles (>250 μm) tend to be free-flowing, whereas fine powders with a high surface area-to-mass ratio become cohesive and tend to stick, especially particles that are less than 10 μm.[12] A small particle size is usually desired for the poorly soluble drug substances with concerns of bioavailability. While it can be challenging to achieve either small or large particle sizes in the crystallization operation, for getting small particles, micronization (e.g., milling) is commonly employed separately for the crystallized solid materials. The current work emphasizes obtaining large particle sizes by crystallization.

For a crystallization process targeting a large particle size, optimized process parameters involve understanding and controlling the underlying mechanisms (e.g., nucleation and growth). For a seeded cooling crystallization in batch, the main parts include optimizing the cooling profile and a seeding strategy. Meanwhile, agitation which renders mixing and mechanical shear is also critical to the final product particle size distribution. The cooling profile significantly impacts the underlying mechanisms, thus affecting a variety of product attributes, such as form, morphology, particle size, etc. Promoting growth mechanisms to achieve a large particle size usually requires a slow cooling rate in a controlled way to maintain the cooling profile within the metastable zone width (MSZW). Seeding is an established technique for improving crystal quality and process robustness, which has been developed for various applications including control of particle

Received: August 31, 2022

size distribution (PSD). Increased particle size can be obtained by using seeds to suppress nucleation and facilitate crystal growth. Mixing by agitation is an important aspect for the crystallization process and significantly impacts particle size distribution as the selection of impeller and agitation rate can affect the process and product attributes. PSD is usually measured using multiple techniques, both inline and offline. Probe-based methods are well-suited for inline "real-time" monitoring of PSD, which has led to improved capability to understand, optimize, and control the crystallization process to achieve target CQAs. However, offline methods are suited for PSD measurement after the downstream operations such as filtration and drying of crystalline material, which could result in agglomeration or breakage of crystals, changing the final PSD obtained from the crystallization process. The discrepancy in PSD measurements arises owing to the physical principles of measurement employed by various methods as well as the sampling location in the process stream.

Targeting particle sizes within certain specifications can be challenging, particularly when trying to produce materials with good flow properties. The inherent thermodynamic and kinetic limitations along with the interplay associated with the critical events, vis-à-vis nucleation, growth, attrition, and agglomeration, leads to convoluted experimental findings. It is beneficial to review the critical factors to be taken into consideration, the relevant strategies used for making large particles by crystallization, as well as the approaches and techniques being applied for various cases. This paper is not on how to grow a large single crystal but rather on increasing the mean particle size in the distribution. Additionally, the current work only summarizes recent approaches focusing on key process parameters including the cooling profile and seeding. Mixing by agitation is also discussed. In addition, a few practical issues such as particle size measurement discrepancies are also addressed.

2. PARTICLE SIZE DISTRIBUTION AND CRYSTALLIZATION KINETICS

The final particle size distribution is governed by the combination of nucleation, growth, breakage, and agglomeration. Nucleation and growth are two fundamental events in crystal formation, of which the interplay and their relations to particle size can be found in many reports.[13−15] For the sole purpose of generating a large particle size, nucleation should be suppressed and growth be dominated (Figure 1). Breakage can be induced by attrition caused by the contact between the propeller and particles inside the reactor vessel, resulting in fine particle generation that leads to a reduced mean particle size. Furthermore, some compounds tend to agglomerate which would increase the particle sizes and can be utilized to achieve higher mean sizes if the agglomeration does not affect the quality attributes (e.g., purity, bioavailability) and downstream processing steps.

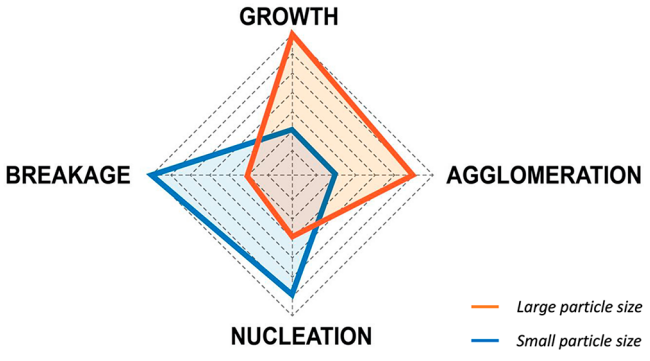

Figure 1. Simple diamond chart illustrates the convoluted events, i.e., nucleation and growth, along with breakage and agglomeration and their influence on particle sizes.

Generally, the interplay of nucleation and crystal growth with respect to particle size distribution can be described by a population balance model (PBM), which has a general expression of

$$\frac{\partial n(t, \mathbf{X})}{\partial t} + \nabla_X[(\mathbf{G_i}n)] + n\frac{d(\log(V))}{dt} = B_{\text{birth}} - D_{\text{death}} - \sum_k \frac{Q_k n_k}{V} \quad (1)$$

where $n(t,\mathbf{X})$ is the number density function, and $\mathbf{G_i}$ denotes the crystal growth rate ($\mathbf{v_i}$). $\mathbf{X} = [\mathbf{x_1}, \mathbf{x_2},...\mathbf{x_N}]$ is the vector containing the various characteristic lengths. B_{birth} is the birth rate, D_{death} is the crystal death rate, V is the volume of the crystallization solution, and Q_k is the volumetric flow rate which describes the volumetric change due to inlet and outlet to the crystallization solution; i.e., V and Q_k must have the same basis.

For the batch and continuous crystallizers that are well-mixed (at both macroscale and microscale levels), unseeded, and with no agglomeration or breakage phenomena, the PBMs with the corresponding initial (I.C.) and boundary conditions (B.C.) can be expressed, respectively, by the following.

Batch:

$$\frac{\partial n(t, \mathbf{X})}{\partial t} + \nabla_X[\mathbf{G}_i n(t, \mathbf{X})] = B\delta(\mathbf{X} - \mathbf{X_0}) \quad (2)$$

I.C.:

$$n(\mathbf{X}, t = 0) = 0 \quad (3)$$

B.C.:

$$\lim_{X \to L_n} [\mathbf{G}_1 + \mathbf{G}_2 + ... + \mathbf{G_N}] = 0, \quad X \in \partial\Omega \quad (4)$$

Continuous (MSMPR):

$$\frac{\partial n(t, \mathbf{X})}{\partial t} + \nabla_X[\mathbf{G_i}n(t, \mathbf{X})] = B\delta(\mathbf{X} - \mathbf{X}_0) - \frac{1}{\tau}n(t, \mathbf{X}) \quad (5)$$

I.C.:

$$n(\mathbf{X}, t = 0) = n_0(\mathbf{X}) \quad (6)$$

B.C. 1:

$$\lim_{X \to L_n} [\mathbf{G}_1 n(\mathbf{X}, t) + \mathbf{G}_2 n(\mathbf{X}, t) + ... + \mathbf{G_N} n(\mathbf{X}, t)] = 0, \quad X \in \partial\Omega \quad (7)$$

B.C. 2:

$$\lim_{X \to \infty} n(\mathbf{X}, t) = 0 \quad (8)$$

where B is the nucleation rate and $\mathbf{G_i} = [\mathbf{G_1}, \mathbf{G_2},...,\mathbf{G_N}]$ is the vector of the crystal growth rate of the characteristic crystal facets. $\partial\Omega$ is the boundary of the size space. $\delta(\mathbf{X}-\mathbf{X_0})$ is the

https://doi.org/10.1021/acs.oprd.2c00277
Org. Process Res. Dev. XXXX, XXX, XXX−XXX

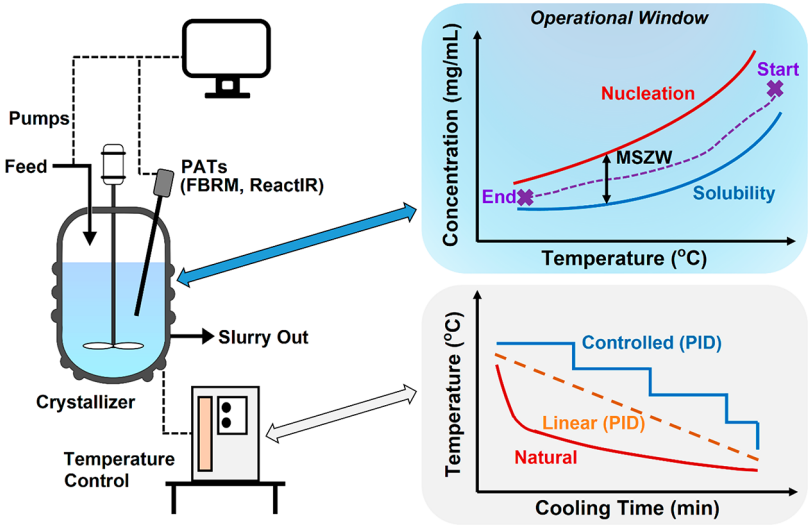

Figure 2. Schematic of experimental setup, equipment, operational window, and temperature profiles for natural, linear, and controlled cooling.

delta distribution that characterizes the formation of the nuclei and is zero for all the values of **X**, except when $\mathbf{X} = \mathbf{X}_0$.

Modeling work has been performed for a variety of systems, including unseeded crystallization, secondary nucleation, temperature cycling, etc.[6,8,16] Li et al. decoupled the primary nucleation, secondary nucleation, and crystal growth for unseeded cooling crystallization (with a preceding temperature plateau) of paracetamol, a commonly studied compound.[6] Using an empirical model for secondary nucleation and fitting data to the PBE, it was found that most crystals resulted from secondary nucleation, which has a rate constant of 1×10^5, whereas that of primary nucleation is 0.2 No./s/kg solvent. An attainable particle size distribution region was proposed by Vetter et al. for three organic compounds in which two compounds (asparagine, aspirin) are growth only and one is considered secondary nucleation (paracetamol).[17]

The population balance model is a strong tool to predict the particle size distribution; however, major limitations originate due to uncertainties to predict the exact mechanism in play for crystallization. It is difficult to have a fully descriptive model, e.g., with respect to obtaining parameters that define the process. In another aspect, there are mathematical and numerical challenges for the events, such as breaking, mixing, and particulate evolution at a higher dimension.[18] Due to nucleation, growth, dissolution, attrition, hydrodynamic, and a mixing profile of different vessels influencing the crystallization process, the model fails to predict the final particle size in many real-world scenarios.

In the context of modeling, process parameters and corresponding results are the subject and in the meantime the object. The sections below discuss a few techniques and critical process parameters that are relevant for obtaining a large particle size.

3. KEY PROCESS PARAMETERS TO OBTAIN LARGE PARTICLE SIZES

For a given compound, the crystallization process and product properties are confined by a range of factors in several aspects—equipment, process parameters, engineering control, etc.[19] A large outcome from the emergence of continuous manufacturing of pharmaceuticals is the development of equipment.[20−24] Jiang et al. summarized the types and the design of crystallizers highlighting continuous-flow crystallization.[25] There is an increased number of cases that have been reported for control of process and product attributes, particularly particle size and size distribution.[26−28] This paper only discusses some of the process parameters that are critical to getting large particles and how they impact the final product in example cases. Below, we divide them into three classes: cooling profile (can be categorized as process kinetic parameters[29]), seeding, and agitation.

3.1. Cooling Profile. *3.1.1. Controlled Cooling/Cubic Cooling.* Cooling is the most common method of crystallization. Alternative methods, such as evaporation and antisolvent addition, can be used individually or in combination. All methods act as a means to generate supersaturation. Control of supersaturation may be realized by employing the appropriate time profiles for cooling rate, evaporation rate, and antisolvent addition rate.[15] The prominent effect of the cooling rate on particle size was demonstrated by Kim et al., who compared particles subjected to four different cooling rates of 0.1, 0.2, 0.5, and 1.0 °C/min, and they concluded that the particle size is highly dependent and inversely proportional to the cooling rate.[30] Liotta et al. implemented in situ monitoring and process control tools to understand and control the crystallization of an API,[31] for which varying cooling rates and seeding protocols were employed, as well as nonlinear temperature profiles that resulted in crystals of larger size. The particles obtained are significantly larger compared to the particles in experiments without control. Of the two supersaturation set-point values used in their study (a) 2.0 and (b) 1.5, the growth is more pronounced in the $S = 1.5$ case, leading to a larger and more uniform crystal size population. An example of the effect of evaporation rate on the PSD of niflumic acid was demonstrated by Stefanidis et al.[32] Microwave was found to greatly reduce the crystallization time (the time from the solution reaching supersaturation to complete evaporation). Due to the high evaporation rates achieved, which implies high supersaturation ratios and thus high nucleation rates, microwave irradiation for evaporative crystallization resulted in the mean volume diameter of 25 μm at the maximum, determined by laser diffraction particle size analysis, whereas in the hot plate experiments (evaporation by heating), the crystal size was

https://doi.org/10.1021/acs.oprd.2c00277
Org. Process Res. Dev. XXXX, XXX, XXX−XXX

found to be around 100 μm in diameter. In addition, microwave-assisted evaporation crystallization resulted in significantly narrower standard deviation in the crystal size. For crystallization involving a reaction or antisolvent, mixing of the feed streams can greatly affect the crystallization process and hence the critical quality attributes such as particle size distribution.[33,34] Additionally, concentration control has been reported in cooling and antisolvent crystallization.[35−37] The adaptive control started cooling until primary nucleation occurred, then adapted to maintain the desired counts/s based on FBRM, able to detect the new metastable zone width which changes with the amount of solids in the slurry, providing fine particle removal with no additional equipment or design needed. The resulting temperature profile showed bursts of increased temperature dissolving excess crystals.[35]

In cooling crystallizations, maintaining the solution concentration profile within the metastable zone and closer to the solubility curve makes the crystal growth dominate the crystallization events (Figure 2). Cubic cooling (slower rate at the beginning and faster rate toward the end) provides a constant supersaturation with an optimized temperature trajectory (Figure 2). The nonlinear temperature trajectory obtained from the laboratory control experiment can be programmed in a larger-scale crystallizer. Linear cooling tends to generate more particles, resulting in a wider size distribution.[38] Development of an optimal cooling profile can be aided by modeling the crystallization process. Worlitschek and Mazzotti examined the supersaturation profile in establishing an optimal route (cubic cooling), which led to a slow increase of supersaturation toward the end of the cooling phase. In contrast, linear cooling led to an inverse profile with a maximum supersaturation at the beginning of the process and a decrease toward the end of the cooling. While the final PSD of the linear cooling is dominated by newly formed nuclei, significantly less nucleation is observed in the case of the optimized crystallization run. The optimized profile ends at a point between of the two cooling profiles with constant supersaturation of 6 and 7 g/kg, respectively, resulting in a PSD similar to that of 6 g/kg without the mode in the smaller size region (evident in 7 g/kg) in a shorter time frame similar to that of 7 g/kg.[39]

Owing to the nucleation and growth rate and their interplay, control of the cooling profile alone may not attain the desired particle size specification. Therefore, other strategies and techniques are often utilized and described later in the study. Despite the aforementioned cases, in practice, the compounds often do not exhibit such preferred behavior, particularly for a nucleation-dominated process with a very slow growth rate. Another problematic scenario is a wide MSZW, which makes it hard to control crystallization generating particles out of spec. External intervention such as sonication and milling can be used to induce nucleation.[40] As pointed out in the previous literature,[1] it can be very challenging to achieve desired physicochemical properties for the compounds in practice; the motivation of the current work is to review and summarize relevant strategies useful to meet these challenges.

3.1.2. Temperature Cycling. Aside from a unidirectional change of temperature (or supersaturation), a change in the reverse direction can be utilized as an alternative approach to minimize unwanted nucleation. Temperature cycling is another technique used to overcome the hurdles in achieving the desired particle size distribution via cooling and heating cycles to eliminate fine particles and promote growth, thus enlarging the mean particle size as well as increasing the particle size uniformity. Typically, in a batch operation, such a profile contains one or several temperature cycles which has a controlled cooling stage followed by a heating stage and ends with a cooling operation. For the continuous mode, such a profile can be implemented in different segments of the system. In a plug flow crystallizer, the different temperature zones can be deployed in each tube segment, rendering temperature cycling to the flowing mother solution.[41] In a MSMPR, such a temperature profile can be implemented using multistage crystallizers, wherein the reactor held at high temperature serves as a dissolution stage. With the aid of process analytical technology (PAT), which provides real-time measurements (e.g., concentration) and mathematical modeling which defines the optimal temperature profile, in situ fine particle removal by temperature cycling that does not require any extra dissolution unit has been shown to work successfully.[39,42−44] However, maintaining such a temperature profile may not completely remove the fine particles. Recycling the slurry through an extra unit with different settings and apparatus (e.g., dissolution vessel, heating pipe, etc.) has been proven to increase the efficiency of fine particle removal.[45−48]

Majumber studied the optimal temperature profiles aiming to yield crystals with target unimodal PSD for various types of growth and dissolution kinetics.[41] Most effective is when both the growth and dissolution kinetics are size-dependent (the larger crystals grow faster than the smaller ones, and the smaller crystals dissolve faster than the larger ones). For the case when both growth and dissolution kinetics are size-independent, the fine particles cannot be reduced to the desired level. When it is size-dependent for only dissolution or growth, a better outcome (compared to both dissolution and growth are size-independent) in terms of fine particle dissolution is expected, but the fine particles that appear at the final stages cannot be removed.

From a similar principle, direct nucleation control (DNC) utilizes thermal cycles and controlled dissolution to eliminate the fine particles in the mother liquor.[49,50] It involves manipulation of temperature and works through a feedback control strategy based on the measurement of particle number in the system. In tackling the challenges arising from the slow growth kinetics of an API with needle-like morphology, Yang et al. applied DNC and in situ immersion milling in producing crystals of larger size and lower aspect ratio.[51] In their study, four approaches were investigated, namely, (1) supersaturation control (SSC), (2) direct nucleation control (DNC), (3) sequential milling−DNC, and (4) simultaneous milling−DNC. Compared to simple unseeded or seeded linear cooling crystallization, it was found that SSC and DNC were able to improve particle size (roughly from 10 to 15 μm). Several supersaturation set-points were compared, and a relative supersaturation of 0.15 was optimal to avoid high nucleation rates, resulting in the largest average size. DNC was a more effective approach to obtain higher quality of crystals aided by in situ dissolution of fine particles, and no complex calibration was required. The results indicated that the average particle length increased significantly in the first two thermal cycles; however, it had a marginal effect in the third and fourth cycles, which was attributed to crystal growth being favored at higher temperatures. In addition, sequential and simultaneous milling−DNC approaches could reduce the particle 2D aspect ratio without generating fine particles, but the simultaneous

https://doi.org/10.1021/acs.oprd.2c00277
Org. Process Res. Dev. XXXX, XXX, XXX−XXX

approach lacks practicality due to the long batch time required to achieve the desired yield.

Eren et al. recently employed temperature cycling to tackle particle size distribution and morphology of a drug compound which had a high aspect ratio and a tendency for primary nucleation.[52] Results showed that the mean size increased with increasing number of temperature cycling, and the particle size distribution was skewed toward the larger sizes after 3 cycles compared to linear cooling and 1 cycle. In another study, an annealing vessel (an extra vessel in the recirculation systems for fine particle dissolution) was used, and wet milling was applied in combination to alter the PSD.[53] A broad, bimodal PSD of an active pharmaceutical ingredient was turned into monodispersed particles in a lab-scale crystallization system in which an annealing step was proven to be significantly effective in eliminating the fine particles, thus shifting the weight of the PSD toward the higher end. Temperature cycling has been increasingly adopted and studied in crystallization development.[54,55] Particle size uniformity has been found to be greatly improved by this approach.[56] Bakar et al. investigated the effect of temperature cycling on the surface features of sulfathiazole crystals, and those features were correlated to focused beam reflectance measurement (FBRM) results.[57] Results showed that temperature cycling combined with membrane seeds was successful in producing large size crystals with narrow PSD and with no visible agglomeration for a highly agglomeration-prone compounds.[58] Production of a larger crystal size with minimal liquid inclusion of cyclotrimethylene trinitramine (RDX, an energetic material) was simultaneously accomplished by Kim et al., who investigated key process parameters including an initial cooling rate, the range of the temperature cycle, and recooling rates of temperature cycling.[30]

3.2. Seeding. Seeding is an effective technique employed to achieve control over the crystallization process and to improve crystal quality and process robustness, particularly in the batch crystallization process.[59−61] Seed crystals, with predetermined amount, form, size, and other properties such as surface area, act as templates for the solute to attach in order to promote a controlled crystallization (Figure 3). The mean size will be critically dependent on the growth phase after seeding. Following growth, secondary nucleation and/or attrition would decrease the mean size of the product. Seeding conditions such as seed load can determine product quality. Addressing those conditions can be a difficult task when designing a crystallization process. A design of experiment will be needed to find the best combination of conditions to achieve the desired product attributes.

3.2.1. Seed Load. Seed load can have a significant impact on the final PSD. It is possibly the most critical parameter that needs to be determined in seeding. Based on previous literature findings, the general range of the seed load is 0.1−10% of theoretical product yield, with some reported up to 15%.[59,62] More seeds can consume the level of supersaturation, facilitate growth, and inhibit nucleation. A case was reported where a 0.2% seed level was clearly insufficient to control the supersaturation, and 2.0% seed gave a smoother crystallization profile.[15] However, it is important to note that there is no simple and universal relation for seed load and product particle size, not to mention the drawbacks in using a large seed load. An optimal seed load needs to be determined.

Different impacts of seed load on particle size have been observed, and it indicates that there is a critical seed load for getting the largest particle size in each process with other

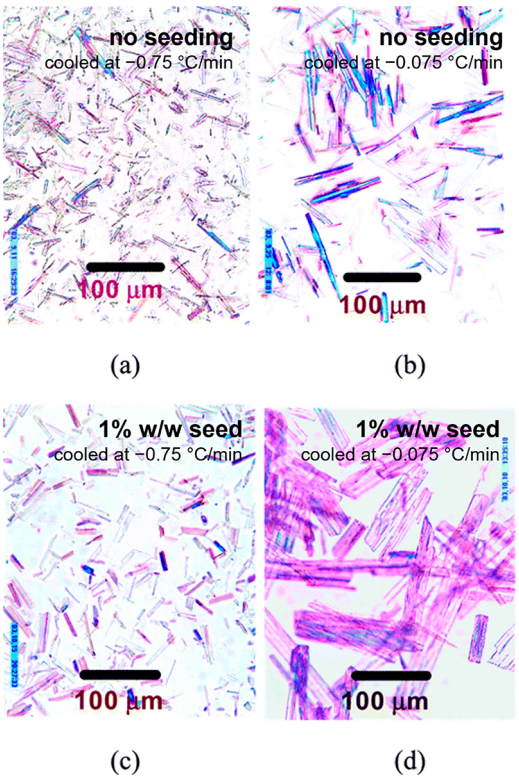

Figure 3. Photomicrographs of a crystalline API candidate from cooling crystallization experiments: (a) cooled at −0.75 °C/min, no seeding; (b) cooled at −0.075 °C/min, no seeding; (c) cooled at −0.75 °C/min, with 1% w/w seed; (d) cooled at −0.075 °C/min, with 1% w/w seed. Reproduced from ref 31. Copyright 2004 American Chemical Society.

parameters fixed. Such a critical load may be subject to change of process parameters (e.g., cooling rate). For a slower cooling rate, the "critical seed load" would be expected to be lower, as less surface area would be needed to keep the system at lower supersaturation. An optimal seed load would minimize nucleation and allow for maximum growth on top of the seeds. Eder et al. found out that, in their system, 0.02 and 0.04 seeding loads (g_{seed}/mL_{slurry}) had nearly identical product particle size, and a 0.05 seed load slightly decreased the mean particle size.[63] Higher seeding load does not necessarily increase the product size. With the same seed size, the effect of seed load of 10, 15, and 20% was investigated in the crystallization of paracetamol, and a decrease in the normalized product size was observed with increased seed loading.[64] The seed load effect on particle size of potassium alum and potassium nitrate was studied by Doki and Huang, respectively.[65,66] Doki et al. proposed a critical seed load above which no secondary nucleation occurs, while Huang reported that with the increasing of seed load, the linear growth rate of a single crystal and the mean size of the products both decreased accordingly. The mechanism in which the large seed load leads to a decreased mean size can be complex, but it is proposed that this is because the theoretical mass of crystals produced could consist of either numerous small crystals or fewer large ones, in which each seed crystal grows to a smaller final size than if there are fewer seeds at the same supersaturation.[64] There are also reported cases where seed load does not have a significant impact on the product PSD.[26] The optimum seed load varies depending on the

https://doi.org/10.1021/acs.oprd.2c00277
Org. Process Res. Dev. XXXX, XXX, XXX−XXX

system and should be studied when developing a process that has PSD as a targeted attribute.

In the studies previously mentioned, separate ways of expressing the seed load were used, hence there is a need to unify the expression of seed load. There are several types of expressions: mass/volume; seed mass/theoretical yield mass; seed mass/dissolved mass. A common expression is the ratio of seed mass to dissolved mass.

Seed load can be related to the product particle size by mass balance. For a growth only model, assuming the same density of seeds and product, and based on mass balance

$$\frac{m_s}{m_p} = \left(\frac{l_s}{l_p}\right)^3 \tag{9}$$

where m_s is mass of the seeds, m_p is mass of the product, l_s and l_p are the diameter of the seed and product particle, respectively (if treated as spherical).

However, this model does not count for secondary nucleation. For several compounds, the extent of secondary nucleation needs to be monitored when developing a crystallization process. With regard to secondary nucleation, we define the ratio of the number of particles formed by secondary nucleation to the number of seed crystals as f.

$$f = \frac{n_{\text{secondary nucleation}}}{n_{\text{seeds}}} \tag{10}$$

Based on mass balance and omitting the deduction process, we have

$$(1+f)\frac{m_s}{m_p} = \left(\frac{l_s}{l_p}\right)^3 \tag{11}$$

3.2.2. Seed Size. As a common strategy, smaller seed crystals are used for crystallization of APIs. There are multiple techniques used for the preparation of seed crystals. Risks associated with a smaller size seed may include agglomeration, which can result in lower purity. However, agglomeration of small seed crystals can be mitigated by size selection and slurry preparation.[67] The smaller seed crystals generally provide larger surface area and facilitate the growth. Additionally, smaller seed crystals were found to have better performance in nucleation inhibition.[68] Coles and Threlfall pointed out that the key seed size may not be about the size but rather the surface effects.[69] To elucidate the effect of seed sizes on product attributes, the other crystallization parameters need to be held constant. Zhang et al. developed an optimized seeding strategy for a seeded cooling process within a certain temperature range based on their calculations.[38] Plotting optimized cooling time against seed size and seed load generated a 3D surface below which it would lead to undesired secondary nucleation, and their results suggested that seed size has a higher impact than seed load on the cooling time, as the total surface area is more sensitive to the seed size. A narrow distribution of seed size is preferred for repeatability. For a growth-dependent crystallization, the cooling profiles will not change the dispersion (distribution).[70]

3.3. Effect of Agitation on Particle Sizes. The size of crystals obtained during crystallization are greatly affected by the hydrodynamic conditions of mixing in the crystallizer.[71] In a typical crystallization process, the generation of supersaturation (cooling, evaporation, antisolvent) and its spatial and temporal distribution in the reactor is affected by macro- and micromixing (at molecular scale).[72] Micromixing is most important for reactive or additive crystallization. Reactive or additive crystallization involves the reaction of two reagents to form the solute that crystallizes out as the product. The three subprocesses for crystallization, namely, chemical reaction, nucleation, and growth, occur at a molecular level and the effect of mixing on these processes must be considered while targeting a specified PSD for crystals. Micromixing can be approximated by comparing characteristic times for precipitation and the chemical reaction; if the time for micromixing is lower than the reaction time, then the reactor would achieve homogeneous composition and nucleation kinetics would control the process.[15] Although many different reactors are used for crystallization, the influence of mixing on PSD in a mixed-suspension mixed-product removal (MSMPR) crystallizer will be discussed in this review. Different scales of mixing are important to homogeneity in an MSMPR, but cooling crystallization is usually dependent on mixing at larger length scales. The MSMPR uses an appropriately designed mixer to achieve sufficient mixing so that the slurry (mother liquor and solids) are spatially homogeneous in the reactor and have the same particle size distribution as the spatially averaged PSD.[73] The common impeller types (Figure 4) used in a MSMPR include pitched-blade turbine, flat-blade turbine, curved-blade turbine, rushton turbine, hydrofoil, retreat curve, propeller, and anchor-type geometry.[74] The choice of using a specific impeller is determined based on its ability to achieve a homogeneous and fast mixing of the incoming feed in the bulk suspension and help with efficient heat transfer. Moreover, the shear forces from the agitator should not result in attrition of the growing crystals or lead to excessive secondary nucleation, which may result in poor control of PSD.

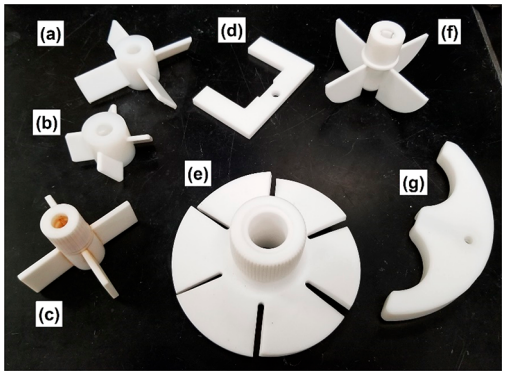

Figure 4. Different impeller designs used in crystallizers: (a,b) pitched-blade turbine, (c) flat-blade turbine, (d) flat-two-blade paddle, (e) flat disk impeller, (f) anchor-type (four blade) impeller, and (g) anchor-type (half-moon) impeller.

In larger volume reactor vessels, multiple impellers (radial and axial) are typically used to keep the solids moving smoothly in the reactor and provide high shear regions in the vicinity of the injection point for the feed. All impellers on a single shaft system need to act in concert so that flow from one impeller feeds smoothly into the next for efficient mixing, without any dead zones.[75] Additionally, the use of baffles in the reactor helps convert much of the tangential flow originating from the impeller to axial flow, which is required for crystal suspension and macromixing. A small gap is usually left between the reactor wall and the baffle to allow for the flow of

https://doi.org/10.1021/acs.oprd.2c00277
Org. Process Res. Dev. XXXX, XXX, XXX−XXX

material and prevent any fouling in the vessel. In order to achieve similar yields and PSD while scaling-up crystallization processes, efficient mixing characteristics need to be ensured in a larger volume reactor.[76] Mixing scale-up can be considered in three primary ways—*geometrically*, where the vessel and agitation configuration maintain the same shape and relative sizes (aspect ratios), *kinematically*, where the relative velocities are maintained, and *dynamically*, where the relative forces are maintained. While batch reactors are still predominantly used for crystallization in the pharmaceutical industry, there is a slow trend toward instituting continuous processing.

Liu et al.[77] reported the influence of agitation (stirring rpm, type of impeller, and baffles) on induction time of butyl paraben dissolved in ethanol solution. They measured induction times at different supersaturations and temperatures in three different jacketed vessels that used overhead stirring. The induction time is defined as the time period (or lag) between the creation of supersaturation and the detection of the first crystals appearing in the mother liquor. A high-resolution camera is typically used for recording the process of crystallization in the reactor and estimation of induction time; the mother liquor turns turbid shortly after the onset of primary nucleation. They used a marine propeller, a rushton turbine, and a disk type of impeller and found that induction times were shortest for the rushton turbine at all rpms, followed by a marine propeller and then the disk impeller. The presence of baffles lowered the induction times when used in conjunction with the rushton turbine and had minimal influence on induction times with disk impellers. A larger diameter disk impeller had shorter induction times compared to those of a smaller diameter disk impeller, while other parameters were held constant; the primary reason for this observation was due to higher tip speeds achieved with a larger diameter impeller. For all of the conditions investigated, induction times decreased with increasing agitation rate, as the width of the metastable zone is narrowed.[78] Based on the energy dissipation rate for Taylor−Couette experiments, an empirical relationship was derived which suggested that the rate of nucleation increases with increasing average energy dissipation rate raised to the power 0.3 and shear rate raised to the power 0.6. In certain cases, agitation speed may also favor crystallization of one polymorph over the other.[79]

Ćosić et al.[80] investigated the influence of different inclination angles (30−90°) of a pithed-blade turbine on nucleation and crystal growth kinetics of borax decahydrate in cooling crystallization. The liquid height in the reactor was equal to the diameter of the vessel; the impeller diameter was half the size of the vessel diameter, and the off-bottom clearance was maintained at 1/3 of the height of the liquid. They reported that an increase in the angle from 30 to 90° to the horizontal axis increases the secondary circulating flow below the impeller accompanied by a transition from an axial to a radial flow direction, and a low mixing zone appears in the upper layer of fluid in the reactor. Although the nucleation rate depends on the level of supersaturation, the width of metastable zone decreases with an increase in the impeller blade angle, and the dominant mechanism is primary nucleation caused by the impeller. In mixing regions with turbulent flow, crystal growth rate is limited by the integration of precursor species into the growing nucleation sites. They also reported that larger crystal sizes were obtained at lower blade angles and were more agglomerated compared to smaller crystal sizes at higher blade angles and less agglomerated crystals. Particle agglomeration was addressed as a two-step process: (1) aggregation (two or more crystals collide and remain fused after the collision) and (2) cementation and growth of crystals. The first step is accomplished around the vicinity of the impeller, while the cementation and growth of the agglomerates take place in the upper zone with lower intensity of circulation currents. At angles above 45°, the radial flow becomes more pronounced, leading to higher shear forces that may prevent cementation of crystals.[81] They also observed that the presence of fine particles owing to secondary nucleation and higher supersaturation levels remains the same for all blade angles, while attrition due to mechanical impact between crystal collisions and crystal-blade collision (contact nucleation) increases with higher blade angles. Higher yields were reported for crystallizers with larger impeller blade angles.

Rane et al.[82] explored the effect of impeller design and power consumption (per unit mass) on crystal size distribution (CSD) in a 500 mL stirred tank reactor. They also used computational fluid dynamics (CFD) simulations to predict flow inhomogeneities for three different impeller designs (disc turbine, pitched-blade turbine, and marine propeller), rotated at three speed set points (2.5, 5, and 10 rps). The CFD data were validated against experimental data obtained from phase Doppler particle analyzer (PDPA). Impeller speed is a major factor governing the fluid flow and crystallization process in the crystallizer. Higher speeds tend to homogenize the concentration of the reaction mixture and result in a narrower CSD. They reported that at lower impeller speeds (2.5 rps) the CSD becomes wider owing to low evaporation rate, while higher impeller speeds (10 rps) resulted in a uniform suspension density for each crystal size, leading to a narrow CSD. Higher impeller speeds result in three important effects: (1) enhancement of the nucleation rate resulting in more viable nucleation sites in the crystallizer reducing the average CSD, (2) higher rate of collisions (crystal−crystal and crystal−impeller) resulting in higher attrition and limited opportunity for sustained crystal growth, and (3) an increase in specific power input (watts) improves mixing and homogeneity in mother liquor composition creating a near-constant supersaturation in the crystallizer. Appropriate trade-offs must be made to achieve good mixing while minimizing attrition and limiting secondary nucleation to achieve desired CSD. They also reported that CSD was narrowest for the disk turbine and the widest for the marine propeller, which corresponds to the distribution of energy dissipation rate by the impellers. Across all configurations tested, the CSD is directly related to the distribution of energy dissipation rate in the crystallizer, and the mean crystal size depends on mean power consumption. Mitchell et al.[83] studied nucleation kinetics based on Kubota's theory for cooling crystallization of paracetamol in ethanol solutions and found that induction times decreased with increased levels of agitation as well as with the use of baffles in the reaction vessel. They used a 1 L borosilicate jacketed reactor and an overhead motor for agitator (pitched-blade turbine with four blades at 45°). An unbaffled reactor vessel is prone to solid body rotation wherein the fluid rotates like a solid mass with minimal mixing and an increased agitation creates a large surface vortex, causing entrainment of air bubbles that can inhibit the nucleation process. The baffles maximize power input in the fluid, hinder the formation of surface vortex, and minimize solid body rotation, thereby enhancing the mixing regime. Based on the FBRM measure-

https://doi.org/10.1021/acs.oprd.2c00277
Org. Process Res. Dev. XXXX, XXX, XXX−XXX

ments for estimating induction time, they reported that lower induction times can be attributed to combined effects of increased power input and increased surface area in contact with the solution. For the paracetamol−ethanol system, there was a linear relationship between higher levels of agitation and shorter induction times. O'Grady et al.[78] investigated the effects of antisolvent addition rate and agitation speed on the width of metastable zone using FBRM in a 500 mL reactor. Across all conditions explored, the width of the metastable zone widened with an increased addition rate of antisolvent, and these effects were more pronounced when the addition was closer to the impeller primarily due to efficient mixing. Addition of antisolvent closer to the impeller resulted in rapid incorporation into the bulk mother liquor, leading to repeatable crystallization results; however, for additions closer to the reactor wall, the incorporation is hindered by unfavorable mixing conditions, leading to premature nucleation and more variability. They also reported that, with increased agitation rates, antisolvent addition closer to the impeller leads to a narrower MSZW, possibly due to the increased probability of contact between solute molecules. However, under higher agitation rates, antisolvent addition closer to the wall resulted in a wider MSZW and a corresponding improvement in batch-to-batch repeatability. This observation can be explained by the fact that increased agitation can dissipate local areas of supersaturation, creating a uniform supersaturation and repeatable results. Tizbin et al.[84] performed a CFD analysis to study particulate flow inside a forced circulation crystallizer using the geometry of a small-scale industrial crystallizer. Their study was the first to model interparticle interactions such as breakage (attrition), aggregation, and kinetics (growth model), which leads to a deeper understanding of the PSD variations in the crystallizer. They reported that mean crystal sizes increased by 15.5% inside the boiling and mixing zone, while circulation of crystals in the rest of the crystallizer body had little effect in increasing particle sizes. Changing the input flow rate of the reaction mixture could increase or decrease the outlet particle size depending on the interaction mechanisms of the particles in the crystallizer.

As seen from the summary provided in this section, the phenomenon of mixing in crystallizers is complex, and it may be necessary to optimize mixing conditions (impeller type, speed, etc.) for different reactor sizes to achieve reproducible PSD in a scale-up environment. Some of the factors that greatly improve with better mixing in a MSMPR include fast heat transfer, homogenized composition of the mother liquor (during antisolvent or reagent addition), uniform crystal suspension, etc., while greater mixing intensity also could result in narrowing the MSZW, higher attrition or crystal breakage, greater secondary nucleation that results in lower average particle sizes, and a broader PSD, which may be undesirable. However, in practice, the desired outcome from the crystallization process such as a specific PSD, yield, bulk turnover, among others would dictate the choice for using certain mixing conditions. Risks associated with above-mentioned process parameters regarding the particle size are listed in Table 1.

Table 1. Risks Associated with the Process Parameters Regarding the Particle Size

process parameters	low	high
cooling rate (°C/min)	low throughput	oiling out, uncontrolled nucleation, suppressed growth
seed load (wt %)	rapid seed dissolution, insufficient growth	low yield, secondary nucleation, decreased mean size due to large number of particles
seed size (μm)	agglomeration, impurity	relatively low surface area, secondary nucleation
stirring rate (rpm)	poor mixing, regions with high local supersaturation	attrition, secondary nucleation

4. DISCREPANCY IN PARTICLE SIZE DISTRIBUTION MEASUREMENTS

Physical properties of the API such as particle morphology have a significant impact when developing a drug product with desired CQAs.[85] Drug particle shape can affect downstream processability and cause physical characterization difficulties and drug product performance issues such as a poor dissolution rate or bioavailability.[86] Particle shape and size can affect content and dose uniformity in oral solid dosage (OSD) forms, the grittiness of solid particles in chewable tablets, and other properties related to physicochemical stability.[87] When scaling from pilot plant to manufacturing, it is necessary to meet the regulatory requirement that the final bulk drug substance at both scales must duplicate CQAs including particle size distribution, bulk density, and/or surface area within narrow ranges.[88] This places great demand on accurate PSD measurement of APIs while using various PAT tools and mitigation of errors.

Based on the final drug product specification, the crystallization process for drug substance can be modulated to synthesize target API with small particle sizes ($D_v90 < 10$ μm) or larger particles ($D_v90 > 1000$ μm).[89] The particle size is the property most frequently monitored during the pharmaceutical development and manufacturing process. If the crystallization process produces larger particles, downstream processing (DSP) involving milling operations can be used to achieve desired PSD and shape solubility kinetics. The narrower the PSD range thereby leads to in-spec/on-target manufactured product. Any differences in the crystallization process pertaining to synthesis, reactor scale-up, and optimization of synthesis conditions might lead to differences in crystal growth kinetics and/or the formation of the agglomeration of different strength and sizes. During the process development standpoint, PSD is usually evaluated using more than one method. Conventionally, offline particle size analyzers such as laser diffraction, dynamic light scattering, and sieve analysis were used for product quality control which would require ∼100 mg or several grams of valuable sample for the measurement. However, probe-based methods such as FBRM and particle vision and measurement (PVM) are well-suited for online "real-time" monitoring of PSD, which has led to improved ability for in-process control and to optimize the crystallization process to achieve target CQAs.[90−92] Moreover, DSP operations comprising filtration, washing and drying of API crystals could result in agglomeration or breakage of crystals, changing the final PSD obtained from the process.[93]

Li et al.[94] analyzed PSD for spherical glass beads and nonspherical silica flakes using image analysis (IA), laser diffraction (LD), ultrasonic attenuation spectroscopy (UAS), and FBRM. The conversion between PSDs obtained by IA, LD, and UAS are based on particle shape factors and could widely vary based on the morphology of the API crystals. They reported that particle shape strongly affects the measured distribution. For instance, PSDs measured by IA, LD, and UAS

https://doi.org/10.1021/acs.oprd.2c00277
Org. Process Res. Dev. XXXX, XXX, XXX−XXX

agree well; however, there was no consistency in PSD results for nonspherical particles. IA offers the ability to measure PSD using a high-resolution camera and can be used as an online method to image particles in a dynamic system. The downside for IA is that a significant number of particles must be measured for robust results. On similar lines, UAS measurement is based on the interactions between suspended particles in a suitable solvent and an ultrasonic wave, which utilizes fundamental equations of mass, momentum, and energy. A marked advantage of UAS is the ability of characterize optically opaque particles in concentrated systems with ∼70% volume fraction without a need for dilution. UAS also requires a detailed set of physical properties for the solid and liquid phase, such as thermal dilation (K^{-1}), shear rigidity ($N{\cdot}m^{-2}$), attenuation ($dB{\cdot}m^{-1}$), speed of sound ($m{\cdot}s^{-1}$) etc., which may be difficult to obtain. FBRM measures chord length distributions (CLD) by scanning particles passing in front of the sapphire window, using a focused beam of laser light rotated at a fixed speed.[95] Although FBRM is the most common PAT used for online and inline measurements, it often is subjected to fouling, leading to errors in measurement. Designing or optimizing a process solely based on CLD data to estimate PSD should be carefully used and cross-validated as CLD data depend on optical properties of the particle, morphology, and perturbances in the process (such as fouling, bubble formation on the probe, etc.).[96] LD measures particle size distributions by measuring the angular variation in intensity of light scattered as a laser beam passes through a particulate sample dispersed in a liquid or fluidized in a gas.[97] Large particles scatter light at small angles relative to the laser beam, and small particles scatter light at large angles. The angular scattering intensity data is then analyzed to calculate PSD using Mie theory of scattering. LD reports PSD as a volume equivalent sphere diameter irrespective of particle shape, and measurement errors start compounding for relatively transparent particles below 50 μm. Narang et al.[98] studied CLD for microcrystalline cellulose (MCC) obtained by FBRM and its correlation with offline particle sizing techniques such as sieve analysis, LD, and optical microscopy. Their results concluded that FBRM provided adequate resolution and reproducible measurements for the high shear wet granulation (HSWG) process compared to offline techniques. However, the PSD data obtained by all methods correlated well. Robust utilization of PATs in pharmaceutical unit operations requires a coherent understanding of the interaction of instrumentation and process variables that can impact the resolution and sensitivity to changes in material properties. Zidan et al.[99] employed FBRM along with particle vision and measurement (PVM) for monitoring CLD of microparticle manufacturing of poly(lactide-*co*-glycolide). They reported that FBRM was sensitive to the amount of the solid materials and the number of microparticles formed; however, the use of PVM imaging was imperative to detect various stages of microemulsion droplets, sheath formation, and solidification with subsequent microparticle hardening. They illustrated the synergistic utility of FBRM and PVM in monitoring the progress of particle formation during drug encapsulation. Heath et al.[100] compared the FBRM response with conventional PSD measurement techniques from laser diffraction and electrical sensing zone for a range of sieved aluminum and calcite suspensions. They reported that the mode average of square-weighted chord length was comparable to other sizing methods in a range of 50−400 μm. The square-weighted FBRM results were unaffected by flow velocity of the suspension and the solid fraction in the range of 0.1−20%. They found that lower weighting increases the instrument's susceptibility to changes in solid fraction, while larger particles may be difficult to size accurately due to obscuration by fine particles or due to poor correlation between total particle counts and solid fraction, which can be rectified by corrections to the instrument dead time. Phillips et al.[101] reported that FBRM oversized small particles (<150 μm) and undersized larger particles (>500 μm) while characterizing fine-grained deposits in the river basin.

Hirschle et al.[102] provided an account for PSD discrepancies when measuring particles below 1 μm with various characterization tools along with the advantages and disadvantages of each method. They divided measurement techniques into two categories, depending on whether the samples are analyzed in a wet state (dispersed in a solution) or are in a dry state (powder). The samples analyzed in a dry state tend to agglomerate as the nanoparticles agglomerate to minimize surface energy, and it becomes difficult to identify the primary particle sizes.[103−107] Additionally, X-ray diffraction (XRD) measurements are employed to estimate particle sizes by using the Scherrer equation, which correlates crystal sizes with peak broadening in the patterns.[108] XRD measurements provide the size of diffracting domains inside the crystal rather than the true size of the crystal.[109,110] The lower the number of defects in the structure, a more accurate prediction of the crystal sizes is obtained by XRD. The peak width in the XRD pattern is sensitive to defects in the crystal structure, and the presence of amorphous material tends to reduce the crystalline domain size to lower values compared to the average particle sizes. Acevedo et al.[111] presented models for conversion of CLD to PSD for nonspherical using FBRM and compared the distribution to offline LD measurements. However, the models developed did not consider the impact of agitation speed on the FBRM, which should be evaluated after the process conditions are fully optimized. Figure 5 provides a particle size comparison between measurements from LD and FBRM for an API with bipyramidal crystal morphology. The API was synthesized using cooling crystallization process in a single-stage MSMPR (100 mL) with 200 rpm stirring speed of the PTFE agitator to promote downmixing. The reactor was temperature controlled using a heating jacket connected to a thermoregulator (Huber

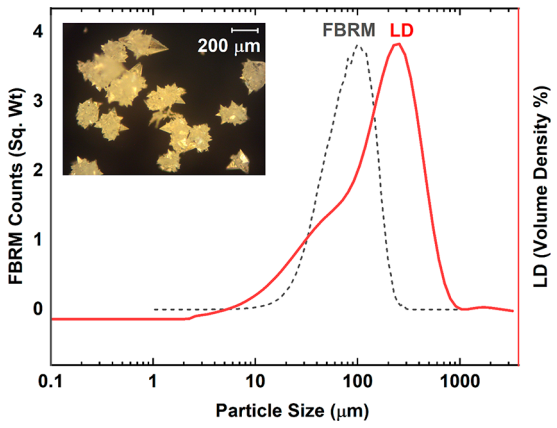

Figure 5. Optical microscopy image (inset) for an API showing bipyramidal crystal morphology and comparison of particle sizes obtained using inline (FBRM) and offline (LD) measurements.

https://doi.org/10.1021/acs.oprd.2c00277
Org. Process Res. Dev. XXXX, XXX, XXX−XXX

Unistat Tango) with a PID controller. The Lasentec FBRM probe was inserted above the PTFE agitator at a 45° angle vertically, which helps prevent the formation of stationary air bubbles resulting in measurement errors. A sampling time of 10 s and an average of 11 measurements were used. The crystallized API samples were filtered using a Buchner funnel with a fritted disc, followed by washing with a benign solvent to remove impurities and dried at 50 °C before LD measurements. The Mastersizer 3000 fitted with Aero M module was used to obtain dry powder dispersion for particle size measurements. Particle sizes obtained by FBRM shows a mode ∼105 μm with a near-Gaussian distribution, while LD shows a mode of ∼255 μm and a left-skewed distribution toward smaller particle sizes. This discrepancy seen in the results originates from the measurement and process conditions used for the instruments. FBRM monitors particles suspended in the mother liquor during crystallization which directly pass in front of the sapphire window. Parameters such as the type of agitator (half-moon, angled pitch-blade, rushton turbine, etc.), the agitator RPM, insertion depth of the FBRM probe, and its subsequent fouling would affect the measurements. Moreover, the square-weighted distribution emphasizes the relative contribution of large chord lengths (>100 μm), while no weighted distribution highlights the contribution from smaller particles (<100 μm), which can further skew the results.[112] The dynamic nature of the crystallization process in the reactor (primary and secondary nucleation, crystal growth) can change the CLD obtained by FBRM as a function of time, which can be effectively used for online process monitoring rather than obtaining a final PSD for the API. Alternatively, offline measurements using LD measures particle sizes postprocess, which could entail particle breakage and agglomeration. LD measurements would represent an actual PSD for the sample at this stage of the process as the API (drug substance) is transformed into a drug product, especially the OSD forms. During end-to-end process development, using FBRM results to design of DSPs such as milling, extrusion, tableting, etc., would result in out-of-specification drug products.[113] PSD methods are process-related, and the crystallization process along with sampling methods should be fine-tuned to support PSD and morphology changes until the process for synthesis, workup, and isolation of the target API is fully established. Continuously monitoring PSD and collecting data, including microscopy, is a part of analytical quality by design (AQbD) approach to develop a robust method that can be validated as required.[114]

5. CONCLUSION

Producing large crystal sizes can be a challenging task during the crystallization process development of a pharmaceutical compound. Unlike the screening stages, where the crystals can be left undisturbed to grow, the crystallization process development in a reactor involves the presence of particles in the mother liquor suspension that is subjected to external effects such as agitation. Most processes developed in the lab will ultimately need to be scaled up and transferred for cGMP manufacturing; thus, the impact and risk associated with translation of the crystallization process parameters needs to be thoroughly investigated. Interplay between nucleation, growth, along with breakage and agglomeration can significantly influence the particle size distribution. Secondary nucleation can be a predominant event reducing the mean particle size and needs to be accounted for. A combination of proper techniques and optimized parameters could result in achieving the target PSD.

The crystallization process has multiple subevents (vis-à-vis nucleation, attrition, etc.) that have several dependent variables, and the operational parameters may influence on single or multiple events. The process parameters were summarized in three main sections, namely cooling profile, seeding and agitation. A combinatorial approach of these process parameters along with inline PAT can be used to suppress unwanted nucleation and promote growth to convert large number of small particles to large particles. Seeding, is a common strategy in directing the crystallization toward a desired outcome, yet much remains unexplored e.g., establishing the optimal seeding condition (primarily seed load and size) in which the microstructure may determine the bulk property. To account for secondary nucleation, we described a simplified expression of seed load, degree of secondary nucleation and product size. Agitation induced mixing by the mechanical impact of the stirrer has complex effects on crystallization, e.g., change of induction time and MSZW and PSD, which has been found to correlate with energy dissipation. Trade-offs might be made in choosing the operating conditions, for higher homogeneity in the solution, thus narrower distribution maybe wanted but not attrition or nucleation. PSD measurements using methods such as laser diffraction, sieve analysis, or light scattering have their own merits along the process development for monitoring product quality. Understanding the discrepancies in different particle size measurement methods is important to choose specific PAT methods during process development. To overcome the challenges in practice, mechanistic studies and application of a diverse set of PAT tools are valuable to improve our understanding of the process and achieve control over the product attributes.

AUTHOR INFORMATION

Corresponding Authors

Fan Liu − *Jiangsu Key Laboratory of Neuropsychiatric Diseases, College of Pharmaceutical Sciences, Soochow University, Suzhou 215123, China; CONTINUUS Pharmaceuticals, Woburn, Massachusetts 01801, United States;* orcid.org/0000-0002-9880-7720; Email: fl362@outlook.com

Salvatore Mascia − *CONTINUUS Pharmaceuticals, Woburn, Massachusetts 01801, United States*; Email: smascia@continuuspharma.com

Authors

Sujay D. Bagi − *CONTINUUS Pharmaceuticals, Woburn, Massachusetts 01801, United States;* orcid.org/0000-0001-7028-190X

Qinglin Su − *CONTINUUS Pharmaceuticals, Woburn, Massachusetts 01801, United States*

Rajshree Chakrabarti − *CONTINUUS Pharmaceuticals, Woburn, Massachusetts 01801, United States*

Rita Barral − *CONTINUUS Pharmaceuticals, Woburn, Massachusetts 01801, United States*

Janaka C. Gamekkanda − *CONTINUUS Pharmaceuticals, Woburn, Massachusetts 01801, United States;* orcid.org/0000-0003-1456-7609

Chuntian Hu − *CONTINUUS Pharmaceuticals, Woburn, Massachusetts 01801, United States;* orcid.org/0000-0002-4232-579X

https://doi.org/10.1021/acs.oprd.2c00277
Org. Process Res. Dev. XXXX, XXX, XXX−XXX

Complete contact information is available at:
https://pubs.acs.org/10.1021/acs.oprd.2c00277

Notes

The authors declare no competing financial interest.

■ ACKNOWLEDGMENTS

F.L. thanks Priority Academic Program Development (PAPD) of Jiangsu Higher Education Institutions.

■ REFERENCES

(1) Paul, S.; Taylor, L. J.; Murphy, B.; Krzyzaniak, J. F.; Dawson, N.; Mullarney, M. P.; Meenan, P.; Sun, C. C. Toward a Molecular Understanding of the Impact of Crystal Size and Shape on Punch Sticking. *Mol. Pharmaceutics* **2020**, *17* (4), 1148−1158.
(2) Wang, C.; Paul, S.; Wang, K.; Hu, S.; Sun, C. C. Relationships among Crystal Structures, Mechanical Properties, and Tableting Performance Probed Using Four Salts of Diphenhydramine. *Cryst. Growth Des.* **2017**, *17* (11), 6030−6040.
(3) Liu, F.; Hooks, D. E.; Li, N.; Mara, N. A.; Swift, J. A. Mechanical Properties of Anhydrous and Hydrated Uric Acid Crystals. *Chem. Mater.* **2018**, *30* (11), 3798−3805.
(4) Liu, F.; Hooks, D. E.; Li, N.; Rubinson, J. F.; Wacker, J. N.; Swift, J. A. Molecular Crystal Mechanical Properties Altered *via* Dopant Inclusion. *Chem. Mater.* **2020**, *32* (9), 3952−3959.
(5) Rathore, A. S.; Winkle, H. Quality by Design for Biopharmaceuticals. *Nat. Biotechnol.* **2009**, *27* (1), 26−34.
(6) Li, H.; Kawajiri, Y.; Grover, M. A.; Rousseau, R. W. Modeling of Nucleation and Growth Kinetics for Unseeded Batch Cooling Crystallization. *Ind. Eng. Chem. Res.* **2017**, *56* (14), 4060−4073.
(7) Li, H.; Yang, B.-S. Model Evaluation of Particle Breakage Facilitated Process Intensification for Mixed-Suspension-Mixed-Product-Removal (MSMPR) Crystallization. *Chem. Eng. Sci.* **2019**, *207*, 1175−1186.
(8) Grover, M. A.; Griffin, D. J.; Tang, X.; Kim, Y.; Rousseau, R. W. Optimal Feedback Control of Batch Self-Assembly Processes Using Dynamic Programming. *J. Process Control* **2020**, *88*, 32−42.
(9) Szilagyi, B.; Eren, A.; Quon, J. L.; Papageorgiou, C. D.; Nagy, Z. K. Application of Model-Free and Model-Based Quality-by-Control (QbC) for the Efficient Design of Pharmaceutical Crystallization Processes. *Cryst. Growth Des.* **2020**, *20* (6), 3979−3996.
(10) Su, Q.; Rielly, C. D.; Powell, K. A.; Nagy, Z. K. Mathematical Modelling and Experimental Validation of a Novel Periodic Flow Crystallization Using MSMPR Crystallizers. *AIChE J.* **2017**, *63* (4), 1313−1327.
(11) Ghadipasha, N.; Romagnoli, J. A.; Tronci, S.; Baratti, R. A Model-Based Approach for Controlling Particle Size Distribution in Combined Cooling-Antisolvent Crystallization Processes. *Chem. Eng. Sci.* **2018**, *190*, 260−272.
(12) Liu, L. X.; Marziano, I.; Bentham, A. C.; Litster, J. D.; White, E. T.; Howes, T. Effect of Particle Properties on the Flowability of Ibuprofen Powders. *Int. J. Pharm.* **2008**, *362* (1−2), 109−117.
(13) Randolph, A. D.; Larson, M. A.*Theory of Particulate Processes: Analysis and Techniques of Continuous Crystallization*, 2nd ed.; Academic Press: San Diego, CA, 1988.
(14) Jancic, S. J.; Grootscholten, P. A.*Industrial Crystallization*; Springer, 1984.
(15) *Handbook of Industrial Crystallization*, 3rd ed.; Myerson, A. S., Erdemir, D., Lee, A. Y., Eds.; Cambridge University Press: Cambridge, UK, 2019.
(16) Fysikopoulos, D.Model-based optimization of batch- and continuous crystallization processes. Ph.D. Thesis, Loughborough University, 2019; https://core.ac.uk/download/pdf/288356013.pdf.
(17) Vetter, T.; Burcham, C. L.; Doherty, M. F. Regions of Attainable Particle Sizes in Continuous and Batch Crystallization Processes. *Chem. Eng. Sci.* **2014**, *106*, 167−180.
(18) Singh, M.; Ranade, V.; Shardt, O.; Matsoukas, T. Challenges and Opportunities Concerning Numerical Solutions for Population Balances: A Critical Review. *J. Phys. Math. Theor.* **2022**, *55* (38), 383002.
(19) Tung, H.-H. Industrial Perspectives of Pharmaceutical Crystallization. *Org. Process Res. Dev.* **2013**, *17* (3), 445−454.
(20) Hu, C. Reactor Design and Selection for Effective Continuous Manufacturing of Pharmaceuticals. *J. Flow Chem.* **2021**, *11*, 243.
(21) Mascia, S.; Heider, P. L.; Zhang, H.; Lakerveld, R.; Benyahia, B.; Barton, P. I.; Braatz, R. D.; Cooney, C. L.; Evans, J. M. B.; Jamison, T. F.; Jensen, K. F.; Myerson, A. S.; Trout, B. L. End-to-End Continuous Manufacturing of Pharmaceuticals: Integrated Synthesis, Purification, and Final Dosage Formation. *Angew. Chem., Int. Ed.* **2013**, *52* (47), 12359−12363.
(22) Adamo, A.; Beingessner, R. L.; Behnam, M.; Chen, J.; Jamison, T. F.; Jensen, K. F.; Monbaliu, J.-C. M.; Myerson, A. S.; Revalor, E. M.; Snead, D. R.; Stelzer, T.; Weeranoppanant, N.; Wong, S. Y.; Zhang, P. On-Demand Continuous-Flow Production of Pharmaceuticals in a Compact, Reconfigurable System. *Science* **2016**, *352* (6281), 61−67.
(23) Zhang, D.; Xu, S.; Du, S.; Wang, J.; Gong, J. Progress of Pharmaceutical Continuous Crystallization. *Engineering* **2017**, *3* (3), 354−364.
(24) Wang, T.; Lu, H.; Wang, J.; Xiao, Y.; Zhou, Y.; Bao, Y.; Hao, H. Recent Progress of Continuous Crystallization. *J. Ind. Eng. Chem.* **2017**, *54*, 14−29.
(25) Jiang, M.; Braatz, R. D. Designs of Continuous-Flow Pharmaceutical Crystallizers: Developments and Practice. *CrystEngComm* **2019**, *21* (23), 3534−3551.
(26) Rosenbaum, T.; Tan, L.; Dummeldinger, M.; Mitchell, N.; Engstrom, J. Population Balance Modeling To Predict Particle Size Distribution upon Scale-Up of a Combined Antisolvent and Cooling Crystallization of an Active Pharmaceutical Ingredient. *Org. Process Res. Dev.* **2019**, *23* (12), 2666−2677.
(27) Jiang, X.; Lu, D.; Xiao, W.; Ruan, X.; Fang, J.; He, G. Membrane Assisted Cooling Crystallization: Process Model, Nucleation, Metastable Zone, and Crystal Size Distribution. *AIChE J.* **2016**, *62* (3), 829−841.
(28) Sun, L.; Song, Y.; Li, B.; Guan, G.; Jiang, Y. A Modified Method for Modelling, Optimization and Control of an Anti-Solvent Crystallization Process. *Chem. Eng. Sci.* **2020**, *211*, 115253.
(29) McGinty, J.; Yazdanpanah, N.; Price, C.; ter Horst, J. H.; Sefcik, J.Chapter 1. Nucleation and Crystal Growth in Continuous Crystallization. In *The Handbook of Continuous Crystallization*; Yazdanpanah, N., Nagy, Z. K., Eds.; Royal Society of Chemistry: Cambridge, UK, 2020; pp 1−50, DOI: 10.1039/9781788013581-00001.
(30) Kim, J.-W.; Kim, J.-K.; Kim, H.-S.; Koo, K.-K. Application of Internal Seeding and Temperature Cycling for Reduction of Liquid Inclusion in the Crystallization of RDX. *Org. Process Res. Dev.* **2011**, *15* (3), 602−609.
(31) Liotta, V.; Sabesan, V. Monitoring and Feedback Control of Supersaturation Using ATR-FTIR to Produce an Active Pharmaceutical Ingredient of a Desired Crystal Size. *Org. Process Res. Dev.* **2004**, *8* (3), 488−494.
(32) Radacsi, N.; ter Horst, J. H.; Stefanidis, G. D. Microwave-Assisted Evaporative Crystallization of Niflumic Acid for Particle Size Reduction. *Cryst. Growth Des.* **2013**, *13* (10), 4186−4189.
(33) Qu, Y.; Cheng, J.; Mao, Z.-S.; Yang, C. A Perspective Review on Mixing Effect for Modeling and Simulation of Reactive and Antisolvent Crystallization Processes. *React. Chem. Eng.* **2021**, *6* (2), 183−196.
(34) Teychené, S.; Rodríguez-Ruiz, I.; Ramamoorthy, R. K. Reactive Crystallization: From Mixing to Control of Kinetics by Additives. *Curr. Opin. Colloid Interface Sci.* **2020**, *46*, 1−19.
(35) Woo, X. Y.; Nagy, Z. K.; Tan, R. B. H.; Braatz, R. D. Adaptive Concentration Control of Cooling and Antisolvent Crystallization with Laser Backscattering Measurement. *Cryst. Growth Des.* **2009**, *9* (1), 182−191.
(36) Su, Q.; Nagy, Z. K.; Rielly, C. D. Pharmaceutical Crystallisation Processes from Batch to Continuous Operation Using MSMPR

Stages: Modelling, Design, and Control. *Chem. Eng. Process. Process Intensif.* **2015**, *89*, 41−53.
(37) Su, Q.-L.; Braatz, R. D.; Chiu, M.-S. JITL-Based Concentration Control for Semi-Batch PH-Shift Reactive Crystallization of l-Glutamic Acid. *J. Process Control* **2014**, *24* (2), 415−421.
(38) Zhang, D.; Liu, L.; Xu, S.; Du, S.; Dong, W.; Gong, J. Optimization of Cooling Strategy and Seeding by FBRM Analysis of Batch Crystallization. *J. Cryst. Growth* **2018**, *486*, 1−9.
(39) Worlitschek, J.; Mazzotti, M. Model-Based Optimization of Particle Size Distribution in Batch-Cooling Crystallization of Paracetamol. *Cryst. Growth Des.* **2004**, *4* (5), 891−903.
(40) Yang, Y.; Ahmed, B.; Mitchell, C.; Quon, J. L.; Siddique, H.; Houson, I.; Florence, A. J.; Papageorgiou, C. D. Investigation of Wet Milling and Indirect Ultrasound as Means for Controlling Nucleation in the Continuous Crystallization of an Active Pharmaceutical Ingredient. *Org. Process Res. Dev.* **2021**, *25* (9), 2119−2132.
(41) Majumder, A.; Nagy, Z. K. Fines Removal in a Continuous Plug Flow Crystallizer by Optimal Spatial Temperature Profiles with Controlled Dissolution. *AIChE J.* **2013**, *59* (12), 4582−4594.
(42) Saleemi, A. N.; Rielly, C. D.; Nagy, Z. K. Comparative Investigation of Supersaturation and Automated Direct Nucleation Control of Crystal Size Distributions Using ATR-UV/Vis Spectroscopy and FBRM. *Cryst. Growth Des.* **2012**, *12* (4), 1792−1807.
(43) Nagy, Z. K.; Aamir, E. Systematic Design of Supersaturation Controlled Crystallization Processes for Shaping the Crystal Size Distribution Using an Analytical Estimator. *Chem. Eng. Sci.* **2012**, *84*, 656−670.
(44) Hansen, T. B.; Simone, E.; Nagy, Z.; Qu, H. Process Analytical Tools To Control Polymorphism and Particle Size in Batch Crystallization Processes. *Org. Process Res. Dev.* **2017**, *21* (6), 855−865.
(45) Qamar, S.; Peter Elsner, M.; Hussain, I.; Seidel-Morgenstern, A. Seeding Strategies and Residence Time Characteristics of Continuous Preferential Crystallization. *Chem. Eng. Sci.* **2012**, *71*, 5−17.
(46) Binel, P.; Mazzotti, M. Selective Dissolution Process Featuring a Classification Device for the Removal of Fines in Crystallization: Experiments. *Ind. Eng. Chem. Res.* **2021**, *60* (43), 15752−15765.
(47) Salvatori, F.; Binel, P.; Mazzotti, M. Efficient Assessment of Combined Crystallization, Milling, and Dissolution Cycles for Crystal Size and Shape Manipulation. *Chem. Eng. Sci. X* **2019**, *1*, 100004.
(48) Acevedo, D.; Jarmer, D. J.; Burcham, C. L.; Polster, C. S.; Nagy, Z. K. A Continuous Multi-Stage Mixed-Suspension Mixed-Product-Removal Crystallization System with Fines Dissolution. *Chem. Eng. Res. Des.* **2018**, *135*, 112−120.
(49) Saleemi, A.; Rielly, C.; Nagy, Z. K. Automated Direct Nucleation Control for in Situ Dynamic Fines Removal in Batch Cooling Crystallization. *CrystEngComm* **2012**, *14* (6), 2196.
(50) Simone, E.; Zhang, W.; Nagy, Z. K. Application of Process Analytical Technology-Based Feedback Control Strategies To Improve Purity and Size Distribution in Biopharmaceutical Crystallization. *Cryst. Growth Des.* **2015**, *15* (6), 2908−2919.
(51) Yang, Y.; Pal, K.; Koswara, A.; Sun, Q.; Zhang, Y.; Quon, J.; McKeown, R.; Goss, C.; Nagy, Z. K. Application of Feedback Control and in Situ Milling to Improve Particle Size and Shape in the Crystallization of a Slow Growing Needle-like Active Pharmaceutical Ingredient. *Int. J. Pharm.* **2017**, *533* (1), 49−61.
(52) Eren, A.; Szilagyi, B.; Quon, J. L.; Papageorgiou, C. D.; Nagy, Z. K. Experimental Investigation of an Integrated Crystallization and Wet-Milling System with Temperature Cycling to Control the Size and Aspect Ratio of Needle-Shaped Pharmaceutical Crystals. *Cryst. Growth Des.* **2021**, *21* (7), 3981−3993.
(53) Meng, W.; Sirota, E.; Feng, H.; McMullen, J. P.; Codan, L.; Cote, A. S. Effective Control of Crystal Size via an Integrated Crystallization, Wet Milling, and Annealing Recirculation System. *Org. Process Res. Dev.* **2020**, *24* (11), 2639−2650.
(54) Wu, Z.; Yang, S.; Wu, W. Application of Temperature Cycling for Crystal Quality Control during Crystallization. *CrystEngComm* **2016**, *18* (13), 2222−2238.
(55) Yazdanpanah, N.; Testa, C. J.; Perala, S. R. K.; Jensen, K. D.; Braatz, R. D.; Myerson, A. S.; Trout, B. L. Continuous Heterogeneous Crystallization on Excipient Surfaces. *Cryst. Growth Des.* **2017**, *17* (6), 3321−3330.
(56) Kim, S.; Wei, C.; Kiang, S. Crystallization Process Development of an Active Pharmaceutical Ingredient and Particle Engineering via the Use of Ultrasonics and Temperature Cycling. *Org. Process Res. Dev.* **2003**, *7* (6), 997−1001.
(57) Abu Bakar, M. R.; Nagy, Z. K.; Rielly, C. D. Investigation of the Effect of Temperature Cycling on Surface Features of Sulfathiazole Crystals during Seeded Batch Cooling Crystallization. *Cryst. Growth Des.* **2010**, *10* (9), 3892−3900.
(58) Simone, E.; Othman, R.; Vladisavljević, G.; Nagy, Z. Preventing Crystal Agglomeration of Pharmaceutical Crystals Using Temperature Cycling and a Novel Membrane Crystallization Procedure for Seed Crystal Generation. *Pharmaceutics* **2018**, *10* (1), 17.
(59) He, Y.; Gao, Z.; Zhang, T.; Sun, J.; Ma, Y.; Tian, N.; Gong, J. Seeding Techniques and Optimization of Solution Crystallization Processes. *Org. Process Res. Dev.* **2020**, *24* (10), 1839−1849.
(60) Zhang, F.; Shan, B.; Wang, Y.; Zhu, Z.; Yu, Z.-Q.; Ma, C. Y. Progress and Opportunities for Utilizing Seeding Techniques in Crystallization Processes. *Org. Process Res. Dev.* **2021**, *25* (7), 1496−1511.
(61) Ou, X.; Li, X.; Rong, H.; Yu, L.; Lu, M. A General Method for Cultivating Single Crystals from Melt Microdroplets. *Chem. Commun.* **2020**, *56* (69), 9950−9953.
(62) *Pharmaceutical Crystals: Science and Engineering*, 1st ed.; Li, T., Mattei, A., Eds.; John Wiley & Sons: Hoboken, NJ, 2018.
(63) Eder, R. J. P.; Schmitt, E. K.; Grill, J.; Radl, S.; Gruber-Woelfler, H.; Khinast, J. G. Seed Loading Effects on the Mean Crystal Size of Acetylsalicylic Acid in a Continuous-Flow Crystallization Device. *Cryst. Res. Technol.* **2011**, *46* (3), 227−237.
(64) Jiang, M.; Ni, X.-W. Reactive Crystallization of Paracetamol in a Continuous Oscillatory Baffled Reactor. *Org. Process Res. Dev.* **2019**, *23* (5), 882−890.
(65) Doki, N.; Kubota, N.; Yokota, M.; Chianese, A. Determination of Critical Seed Loading Ratio for the Production of Crystals of Uni-Modal Size Distribution in Batch Cooling Crystallization of Potassium Alum. *J. Chem. Eng. Jpn.* **2002**, *35* (7), 670−676.
(66) Huang, D. C.; Liu, W.; Zhao, S. K.; Shi, Y. Q.; Wang, Z. X.; Sun, Y. M. Quantitative Design of Seed Load for Solution Cooling Crystallization Based on Kinetic Analysis. *Chem. Eng. J.* **2010**, *156* (2), 360−365.
(67) Jiang, M.; Wong, M. H.; Zhu, Z.; Zhang, J.; Zhou, L.; Wang, K.; Ford Versypt, A. N.; Si, T.; Hasenberg, L. M.; Li, Y.-E.; Braatz, R. D. Towards Achieving a Flattop Crystal Size Distribution by Continuous Seeding and Controlled Growth. *Chem. Eng. Sci.* **2012**, *77*, 2−9.
(68) Tseng, Y.-T.; Ward, J. D. Critical Seed Loading from Nucleation Kinetics. *AIChE J.* **2014**, *60* (5), 1645−1653.
(69) Coles, S. J.; Threlfall, T. L. A perspective on a century of inert seeds in crystallisation. *CrystEngComm* **2014**, *16* (21), 4355.
(70) Patience, D. B.; Klingenberg, D. J.; Engineering, W. H. R. I. C.; Food, R. W. H. I.; Allen, R. M.; Earl, W. B.; Jordan, P. J.; Abrahamson, J.; Stephen, R.; James; Bruce, D.; Patience; Rawlings, J. B.Crystal Engineering through Particle Size and Shape Monitoring, Modeling, and Control Crystal Engineering through Particle Size and Shape Monitoring, Modeling, and Control Notation 141 Appendix a Model-Predictive Control of Crystallizer Temperature 147; **2002**; https://www.semanticscholar.org/paper/Crystal-Engineering-through-Particle-Size-and-Shape-Patience-Klingenberg/82ce72561b071d60c23da1cd3a1fcea9afbe8c6f (accessed 2022-11-22).
(71) Ashraf Ali, B.; Janiga, G.; Temmel, E.; Seidel-Morgenstern, A.; Thévenin, D. Numerical Analysis of Hydrodynamics and Crystal Motion in a Batch Crystallizer. *J. Cryst. Growth* **2013**, *372*, 219−229.
(72) Garside, J.; Tavare, N. S. Mixing, Reaction and Precipitation: Limits of Micromixing in an MSMPR Crystallizer. *Chem. Eng. Sci.* **1985**, *40* (8), 1485−1493.

https://doi.org/10.1021/acs.oprd.2c00277
Org. Process Res. Dev. XXXX, XXX, XXX−XXX

(73) Jiang, M.; Braatz, R. D. Designs of Continuous-Flow Pharmaceutical Crystallizers: Developments and Practice. *CrystEngComm* **2019**, *21* (23), 3534−3551.
(74) Kaćunić, A.; Akrap, M.; Kuzmanić, N. Effect of Impeller Type and Position in a Batch Cooling Crystallizer on the Growth of Borax Decahydrate Crystals. *Chem. Eng. Res. Des.* **2013**, *91* (2), 274−285.
(75) Dutt, A. K.; Datta, A. Imperfect Mixing and Dead-Zone Effects in Nonlinear Dynamics: Law of Mass Action Revisited. *J. Phys. Chem. A* **1998**, *102* (41), 7981−7983.
(76) McConville, F. X.; Kessler, S. B.Scale-up of Mixing Processes: A Primer. In *Chemical Engineering in the Pharmaceutical Industry*; am Ende, D. J., am Ende, M. T., Eds.; John Wiley & Sons, Inc.: Hoboken, NJ, 2019; pp 241−259, DOI: 10.1002/9781119600800.ch12.
(77) Liu, J.; Svärd, M.; Rasmuson, Å. C. Influence of Agitation on Primary Nucleation in Stirred Tank Crystallizers. *Cryst. Growth Des.* **2015**, *15* (9), 4177−4184.
(78) O'Grady, D.; Barrett, M.; Casey, E.; Glennon, B. The Effect of Mixing on the Metastable Zone Width and Nucleation Kinetics in the Anti-Solvent Crystallization of Benzoic Acid. *Chem. Eng. Res. Des.* **2007**, *85* (7), 945−952.
(79) Liu, J.; Svärd, M.; Rasmuson, Å. C. Influence of Agitation and Fluid Shear on Nucleation of *m* -Hydroxybenzoic Acid Polymorphs. *Cryst. Growth Des.* **2014**, *14* (11), 5521−5531.
(80) Ćosić, M.; Kaćunić, A.; Kuzmanić, N. The Investigation of the Influence of Impeller Blade Inclination on Borax Nucleation and Crystal Growth Kinetics. *Chem. Eng. Commun.* **2016**, *203* (11), 1497−1506.
(81) Yu, Z. Q.; Tan, R. B. H.; Chow, P. S. Effects of Operating Conditions on Agglomeration and Habit of Paracetamol Crystals in Anti-Solvent Crystallization. *J. Cryst. Growth* **2005**, *279* (3−4), 477−488.
(82) Rane, C. V.; Ekambara, K.; Joshi, J. B.; Ramkrishna, D. Effect of Impeller Design and Power Consumption on Crystal Size Distribution. *AIChE J.* **2014**, *60* (10), 3596−3613.
(83) Mitchell, N. A.; Frawley, P. J.; Ó'Ciardhá, C. T. Nucleation Kinetics of Paracetamol−Ethanol Solutions from Induction Time Experiments Using Lasentec FBRM®. *J. Cryst. Growth* **2011**, *321* (1), 91−99.
(84) Tizbin, S.; Jafarian, A.; Darand, J. Numerical Investigation of Hydrodynamics and Crystal Growth in a Forced Circulation Crystallizer. *Desalination* **2020**, *496*, 114739.
(85) Azad, M. A.; Capellades, G.; Wang, A. B.; Klee, D. M.; Hammersmith, G.; Rapp, K.; Brancazio, D.; Myerson, A. S. Impact of Critical Material Attributes (CMAs)-Particle Shape on Miniature Pharmaceutical Unit Operations. *AAPS PharmSciTech* **2021**, *22* (3), 98.
(86) Wilson, D.; Bunker, M.; Milne, D.; Jawor-Baczynska, A.; Powell, A.; Blyth, J.; Streather, D. Particle Engineering of Needle Shaped Crystals by Wet Milling and Temperature Cycling: Optimisation for Roller Compaction. *Powder Technol.* **2018**, *339*, 641−650.
(87) Shekunov, B. Y.; Chattopadhyay, P.; Tong, H. H. Y.; Chow, A. H. L. Particle Size Analysis in Pharmaceutics: Principles, Methods and Applications. *Pharm. Res.* **2007**, *24* (2), 203−227.
(88) Paul, E. L.; Tung, H.-H.; Midler, M. Organic Crystallization Processes. *Powder Technol.* **2005**, *150* (2), 133−143.
(89) Kuriyama, A.; Ozaki, Y. Assessment of Active Pharmaceutical Ingredient Particle Size in Tablets by Raman Chemical Imaging Validated Using Polystyrene Microsphere Size Standards. *AAPS PharmSciTech* **2014**, *15* (2), 375−387.
(90) Li, H.; Kawajiri, Y.; Grover, M. A.; Rousseau, R. W. Application of an Empirical FBRM Model to Estimate Crystal Size Distributions in Batch Crystallization. *Cryst. Growth Des.* **2014**, *14* (2), 607−616.
(91) Li, H.; Grover, M. A.; Kawajiri, Y.; Rousseau, R. W. Development of an Empirical Method Relating Crystal Size Distributions and FBRM Measurements. *Chem. Eng. Sci.* **2013**, *89*, 142−151.
(92) Ouyang, J.; Wang, J.; Huang, X.; Gao, Y.; Bao, Y.; Wang, Y.; Yin, Q.; Hao, H. Gel Formation and Phase Transformation during the Crystallization of Valnemulin Hydrogen Tartrate. *Ind. Eng. Chem. Res.* **2014**, *53*, 16859.
(93) Muhaimin, M.; Chaerunisaa, A. Y.; Bodmeier, R. Real-Time Particle Size Analysis Using Focused Beam Reflectance Measurement as a Process Analytical Technology Tool for Continuous Microencapsulation Process. *Sci. Rep.* **2021**, *11* (1), 19390.
(94) Li, M.; Wilkinson, D.; Patchigolla, K. Comparison of Particle Size Distributions Measured Using Different Techniques. *Part. Sci. Technol.* **2005**, *23* (3), 265−284.
(95) Kougoulos, E.; Jones, A. G.; Jennings, K. H.; Wood-Kaczmar, M. W. Use of Focused Beam Reflectance Measurement (FBRM) and Process Video Imaging (PVI) in a Modified Mixed Suspension Mixed Product Removal (MSMPR) Cooling Crystallizer. *J. Cryst. Growth* **2005**, *273* (3−4), 529−534.
(96) Helmdach, L.; Pertig, D.; Rüdiger, S.; Lee, K.-S.; Stelzer, T.; Ulrich, J. Bubbles - Trouble-Makers in Crystallizers: Classical Problems during Inline Measurements. *Chem. Eng. Technol.* **2012**, *35*, 1017−1023.
(97) Varga, G.; Gresina, F.; Újvári, G.; Kovács, J.; Szalai, Z. On the Reliability and Comparability of Laser Diffraction Grain Size Measurements of Paleosols in Loess Records. *Sediment. Geol.* **2019**, *389*, 42−53.
(98) Narang, A. S.; Stevens, T.; Hubert, M.; Paruchuri, S.; Macias, K.; Bindra, D.; Gao, Z.; Badawy, S. Resolution and Sensitivity of Inline Focused Beam Reflectance Measurement During Wet Granulation in Pharmaceutically Relevant Particle Size Ranges. *J. Pharm. Sci.* **2016**, *105* (12), 3594−3602.
(99) Zidan, A. S.; Rahman, Z.; Khan, M. A. Online Monitoring of PLGA Microparticles Formation Using Lasentec Focused Beam Reflectance (FBRM) and Particle Video Microscope (PVM). *AAPS J.* **2010**, *12* (3), 254−262.
(100) Heath, A. R.; Fawell, P. D.; Bahri, P. A.; Swift, J. D. Estimating Average Particle Size by Focused Beam Reflectance Measurement (FBRM). *Part. Part. Syst. Charact.* **2002**, *19* (2), 84.
(101) Phillips, J. M.; Walling, D. E. The Particle Size Characteristics of Fine-Grained Channel Deposits in the River Exe Basin, Devon, UK. *Hydrol. Process.* **1999**, *13* (1), 1−19.
(102) Hirschle, P.; Preiß, T.; Auras, F.; Pick, A.; Völkner, J.; Valdepérez, D.; Witte, G.; Parak, W. J.; Rädler, J. O.; Wuttke, S. Exploration of MOF Nanoparticle Sizes Using Various Physical Characterization Methods − Is What You Measure What You Get? *CrystEngComm* **2016**, *18* (23), 4359−4368.
(103) Goesmann, H.; Feldmann, C. Nanoparticulate Functional Materials. *Angew. Chem., Int. Ed.* **2010**, *49* (8), 1362−1395.
(104) Bagi, S.; Sharma, V.; Aswath, P. B. Role of Dispersant on Soot-Induced Wear in Cummins ISB Engine Test. *Carbon* **2018**, *136*, 395−408.
(105) Bagi, S.; Kamp, C. J.; Sharma, V.; Aswath, P. B. Multiscale Characterization of Exhaust and Crankcase Soot Extracted from Heavy-Duty Diesel Engine and Implications for DPF Ash. *Fuel* **2020**, *282*, 118878.
(106) Bagi, S.; Wright, A. M.; Oppenheim, J.; Dinca, M.; Roman-Leshkov, Y. Accelerated Synthesis of a Ni2Cl2(BTDD) Metal−Organic Framework in a Continuous Flow Reactor for Atmospheric Water Capture. *ACS Sustain. Chem. Eng.* **2021**, *9* (11), 3996−4003.
(107) Holder, C. F.; Schaak, R. E. Tutorial on Powder X-Ray Diffraction for Characterizing Nanoscale Materials. *ACS Nano* **2019**, *13* (7), 7359−7365.
(108) Bagi, S.; Wright, A. M.; Oppenheim, J.; Dinca, M.; Roman-Leshkov, Y. Accelerated Synthesis of a Ni2Cl2(BTDD) Metal−Organic Framework in a Continuous Flow Reactor for Atmospheric Water Capture. *ACS Sustain. Chem. Eng.* **2021**, *9* (11), 3996−4003.
(109) Holder, C. F.; Schaak, R. E. Tutorial on Powder X-Ray Diffraction for Characterizing Nanoscale Materials. *ACS Nano* **2019**, *13* (7), 7359−7365.
(110) Bagi, S. D.; Myerson, A. S.; Román-Leshkov, Y. Solvothermal Crystallization Kinetics and Control of Crystal Size Distribution of MOF-808 in a Continuous Flow Reactor. *Cryst. Growth Des.* **2021**, *21* (11), 6529−6536.

https://doi.org/10.1021/acs.oprd.2c00277
Org. Process Res. Dev. XXXX, XXX, XXX−XXX

(111) Acevedo, D.; Wu, W.-L.; Yang, X.; Pavurala, N.; Mohammad, A.; O'Connor, T. F. Evaluation of Focused Beam Reflectance Measurement (FBRM) for Monitoring and Predicting the Crystal Size of Carbamazepine in Crystallization Processes. *CrystEngComm* **2021**, *23* (4), 972−985.
(112) Yu, Z. Q.; Chow, P. S.; Tan, R. B. H. Interpretation of Focused Beam Reflectance Measurement (FBRM) Data via Simulated Crystallization. *Org. Process Res. Dev.* **2008**, *12* (4), 646−654.
(113) Riley, C. M.; Rosanske, T. W.; Reid, G. L.*Specification of Drug Substances and Products: Development and Validation of Analytical Methods*; Elsevier: Amsterdam, 2020.
(114) Holm, P.; Allesø, M.; Bryder, M. C.; Holm, R.Q8(R2): Pharmaceutical Development. In *ICH Quality Guidelines*; Teasdale, A., Elder, D., Nims, R. W., Eds.; John Wiley & Sons, Inc.: Hoboken, NJ, 2017; pp 535−577, DOI: 10.1002/9781118971147.ch20.

https://doi.org/10.1021/acs.oprd.2c00277
Org. Process Res. Dev. XXXX, XXX, XXX−XXX